THE THEMATIC INFORMATION EXTRACTION FROM POLINSAR DATA FOR URBAN PLANNING AND MANAGEMENT

D.Amarsaikhan [a, *], M.Sato [b], M.Ganzorig [a]

[a] Institute of Informatics and RS, Mongolian Academy of Sciences, av.Enkhtaivan-54B, Ulaanbaatar-51, Mongolia
amar64@arvis.ac.mn, ganzorig@arvis.ac.mn
[b] Center for Northeast Asian Studies, Tohoku University, Kawauchi, Aoba-ku, Sendai 980-8576, Japan
sato@cneas.tohoku.ac.jp

Commission VII, WG VII/2

KEY WORDS: Pi-SAR, Polarimetry, Interferometry, Thematic information, Rule-based, Classification

ABSTRACT:

The aim of this study is to demonstrate the use of Pi-SAR (polarimetric and interferometric synthetic aperture radar) data for the extraction of different thematic information for urban planning and management. For this end, different relief topography related thematic information as well as a land cover map are generated from the Pi-SAR data. The thematic maps related to terrain topography are generated from the interferometric information by applying standard procedures, while for the generation of the land cover map, a refined classification algorithm, which integrates both polarimetric and interferometric information is developed. The refined method is based on a hierarchical rule-based approach and it uses a hierarchy of rules describing different conditions under which the actual classification has to be performed. The result of the developed method was compared with the result obtained by the traditional statistical maximum likelihood classification (MLC). It was indicated that Pi-SAR data can be used for generation of different terrain topography related thematic information and the rule-based method containing well constructed rules is a powerful tool in the production of an accurate land cover map.

1. INTRODUCTION

At present, the development stage of remote sensing (RS) is entering a new challenging era, the era of so called polarimetric and interferometric synthetic aperture radar (POLINSAR). The POLINSAR is an advanced imaging radar system that has multifrequency, fully polarimetric and interferometric observation functions (Amarsaikhan and Sato, 2004). Compared to the single frequency polarimetric radar systems, the POLINSAR has a number of advantages, because some objects which are not seen on the image acquired at lower frequency can be seen on the image acquired at higher frequency, meanwhile, the height information about the classes of objects can be provided. This advantage of the POLINSAR can be clearly observed specifically during the analysis of objects in urban environment, where a small area contains a very high variety of changing behaviors in both frequency and polarization.

For urban planning and management, the detailed spatial information can play an important role. For example, such information can be successfully used for many different disciplines including land cover/use change detection, property management, various network related analysis, neighborhood analysis, utility management and many others (Amarsaikhan and Sato, 2003). For proper management of urban environment, it is necessary to integrate (or extract) the information from a wide range of sources and disciplines and compile them within a geographical information system (GIS) and develop a methodology for the effective and efficient usage of the compiled multisource data sets. From the POLINSAR data, it is possible a) to extract the information related to land cover/use class distribution, b) to generate a digital elevation model (DEM), which in turn can be used for generation of different thematic information related to terrain topography. For the extraction of the information related to land cover/use class distribution, different classification methods can be used, while for the generation of a DEM, an interferometric processing should be applied. During the interferometric processing, a coherence image is derived and it can be used as an extra feature for terrain classification.

The aim of this research is to demonstrate the use of the POLINSAR data for the extraction of different thematic information used for urban planning and management. Within the framework of the study, it was assumed that there is a (urban) GIS and there is a need to create new layers extracting different (thematic) information from the existing Pi-SAR data. For this end, different terrain related thematic information as well as a land cover map were generated from the Pi-SAR data. The terrain related thematic maps were generated from the interferometric DEM (InDEM) by applying standard procedures, while for the generation of the land cover map, a refined classification algorithm, that can integrate both polarimetric and interferometric information was developed. The refined method is based on a hierarchical rule-based approach and it uses a hierarchy of rules describing different conditions under which the actual classification has to be performed. In the upper hierarchy, based on the knowledge about scattering characteristics of the selected classes, a set of rules which contains the initial image segmentation procedure and the constraints on spectral parameters and other threshold values were constructed. The rules in the lower hierarchy include

---

* Corresponding author

different constraints on spectral thresholds defined from polarimetric data and spatial thresholds defined from the interferometric information. The result of the developed method was compared with the result obtained by the traditional statistical MLC.

2. TEST SITE AND Pi-SAR DATA SETS

2.1 Test Site

As a test site, the central part of Sendai city located in northern Japan has been selected. The area is about 4.1kmx3.5km and represents complex urban environment. The selected part of the city is characterized by such main classes as high density urban, low density urban, forest, extended vegetated surface, bare ground and water. The high density urban includes mainly tall buildings located in the downtown area, while low density urban includes more residential houses, though there are some tall buildings, too. The forest class consists of different types of deciduous and coniferous trees located in mountainous part of the Botanical Garden. The extended vegetated surface mainly includes grass, but there are also some trees of different types and size. The bare ground includes bare soil, tennis court and other open fields. The water refers to the Hirose River that flows through the Sendai city. The real world views of the available classes are shown in Figure 1(c).
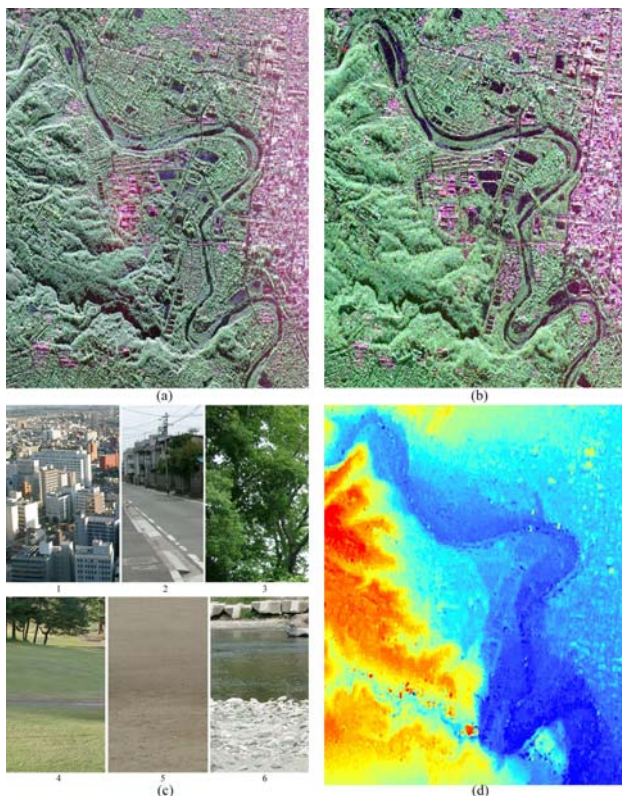

Figure 1. (a) Pi-SAR X-band FCC image (R=HH, G=HV, B=VV), (b) Pi-SAR L-band FCC image (R=HH, G=HV, B=VV), (c) real world views of the available classes: 1-high density urban, 2-low density urban, 3-forest, 4-extended vegetated surface, 5-bare ground, 6-water, (d) the original InDEM (the heights increase from blue to red). The size of the area is about 4.1kmx3.5km.

2.2 Pi-SAR Campaign in Sendai Area

Pi-SAR is an airborne high resolution imaging radar system with fully polarimetric and interferometric functions. The Pi-SAR system was jointly developed by the National Institute of Information and Communications Technology (NICT, former CRL) and the Japan Aerospace Exploration Agency (JAXA, former NASDA). It has fully polarimetric X-band SAR (frequency is 9.55 GHz) and L-band SAR (frequency is 1.27 GHz) and the X-band has two receiving antennas located in cross-track direction for interferometric observation. The X-band image has a spatial resolution of 1.5m, whereas L-band image has a spatial resolution of 3m (Satake *et al.* 2002).

The Pi-SAR has already been operational for several years and acquired a great number of high resolution polarimetric radar images over different test sites in Japan. In Sendai area, the Pi-SAR missions have been performed in August 2001, June 2002, June and August 2003 and February 2004, and the fully polarimetric, multifrequency data were acquired. In the Pi-SAR mission of August 2003, besides the polarimetric imaging, interferometric observation was performed. In this study, fully polarimetric and interferometric Pi-SAR data of 30 August 2003 have been used.

2.3 Geometric Registration of the Pi-SAR Products

To conduct an integrated analysis, the primary Pi-SAR products need to be coregistered. The Pi-SAR DEM used in the present study was provided by the NICT/JAXA. It was generated from the interferometric data sets acquired by the X-band SAR through interferometric processing. For the integration of the interferometric DEM (InDEM) with the polarimetric (intensity) images, firstly the original DEM data represented in a floating point format was converted to an 8 bit image and then it was registered to the coordinates of the L-band image. In order to coregister the coordinates of the InDEM and L-band image, on clearly delineated sites of both images, 12 regularly distributed ground control points (GCP) have been selected and a linear transformation has been applied.

As a resampling technique, nearest neighbour resampling approach was applied and the related rms error was 0.96 pixel. Similarly, the coordinates of the X-band image were transformed to the coordinates of the L-band image. To perform an accurate registration, 24 more regularly distributed GCPs were selected comparing the locations of the selected points on both images. For the transformation, a second order transformation and nearest neighbor resampling approach have been applied and the rms error was 0.98 pixel. The false color composite (FCC) images created by the polarization components of the X-band and L-band data are shown in Figure 1 (a), (b).

3. THE THEMATIC INFORMATION GENERATED FROM THE InDEM

Unlike the ordinary DEM, the InDEM generated from the Pi-SAR data contains the height information of the natural and man-made objects existing on the surface, thus representing the real world view of the scene. The original InDEM is shown in Figure 1 (d). In this study, different thematic information such as slope (a measure of change in surface value over distance, expressed either in degrees or percentage), aspect (indicator of direction towards which a slope faces and measured in degrees starting from 0 degree to the north and angles increasing clockwise direction), contour (isoline representing the equal

surface height value) and shaded relief maps (indicators of shaded and illuminated relieves determined by defining the sun elevation and azimuth) as well as various convexities and curvatures (convexities measure the rate of changes of the slopes and aspects, while curvatures measure the surface curvatures in different directions) were extracted from the InDEM by applying standard procedures (the procedures are based on gray level differentiation of neighboring pixels) (ENVI, 1999). These extracted information were stored as individual layers within a (urban) GIS and when they are integrated with other thematic layers stored in the GIS, can be successfully used for different activities related to research, planning and management.

4. THE RULE-BASED CLASSIFICATION

4.1 Knowledge Acquisition

At present, application of a knowledge-based approach has more and more usage in the automatic interpretation of remote sensing (RS) images. Different types of this approach have been, and are being developed for information extraction from RS images, representing knowledge in different forms. One of the most commonly used knowledge representation technique is the production rule type (Lawrence and Wright, 2001). In the rule-based approach, different rules which mainly contain the constraints on expert-defined variables, spatial objects, external programmes and other spatial models are constructed and used for the hypothesis evaluation (or problem solution) (Amarsaikhan, 2000).

In this study, for discrimination of the land cover classes, a rule-based method, based on a hierarchy of rules that describe different conditions under which the actual classification should be performed, has been developed. For an initial (intelligent) guess of the backscatter return of the selected classes which is important for selecting the reliable features and spectral threshold values, knowledge acquisition was conducted based on the theory of scattering mechanisms of each class available on the Pi-SAR images (Manual of RS, 1998). The initial guess was supported by the statistics of the training samples representing each of the chosen classes and the separability measures evaluated by transformed divergence (TD) (Richards, 1993). The plot of the mean values for the chosen training samples in the selected Pi-SAR polarizations is shown in Figure 2.
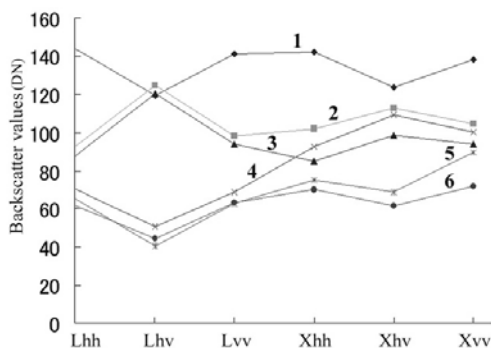

Figure 2. The plot of the mean backscatter values for the available classes. Along the X-axes: PiSAR L- and X-band polarization components. 1-high density urban, 2-low density urban, 3-forest, 4-extended vegetated surface, 5-bare ground, 6-water.

Before conducting any analysis, the speckle of the POLSAR images was suppressed by the use of a 3x3 size Frost filter (ERDAS, 1999). The overall knowledge acquisition process can be formulated as follows:

In general, the backscatter from urban areas should contain information about street alignment, building size, density, roofing material, its orientation as well as vegetation and soil, thus resulting in all kinds of scattering. However, high density urban areas must have very high backscatter due to double bounce effect, while residential areas should have different backscatter return depending on the mixtures of contributing scattering mechanisms. As can be seen from Figure 2, the high density urban class has the highest average backscatter return in all frequencies and polarizations (except in L_{hv}) and it is statistically separable from all classes, whereas the low density urban class has the second highest average backscatter return in all frequencies and polarizations (except in L_{hv}), but it might easily have some overlaps with other classes unless accurate spectral threshold values are selected. In case of forest areas, at X-band frequency, canopy scattering and attenuation will be caused primarily by leaves and needles, while at L-band frequency, the wavelength will penetrate to the forest canopy and will cause volume scattering to be derived by the interactions among twigs, branches, trunks and ground. As seen from Figure 2, the forest has moderate backscatter return and it has a high statistical overlap with the low density urban, specifically in L-band polarizations. Extended vegetated surfaces will act as mixtures of trees, grass and soil and the backscatter will depend on the volume of either of them. In general, the extended vegetated surfaces could have components of diffuse and specular reflection depending on the wavelength and incident angle. At high frequencies, they will be dominated by diffuse scattering, whereas at low frequencies they will be dominated by specular scattering. As seen from the Figure 2, they have higher backscatter return in X-band and there is a high statistical overlap between this class and ground and water classes at L-band frequency. In most cases, bare ground will behave as a specular reflector, but at some specific conditions where sufficient surface roughness is observed, it will have some components of diffuse scattering. As can be seen from Figure 2, compared to most of the other classes, the bare ground has very low average backscatter return and it has a very high statistical overlap with water class. At most radar frequencies, water will behave as a specular reflector and will cause a minimum amount of backscatter return compared to any other classes.

4.2 The Rule-based Algorithm

The developed rule-based algorithm consists of 2 main hierarchies. In the upper hierarchy, on the basis of knowledge about scattering characteristics of the selected six classes, a set of rules which contains the initial image segmentation procedure based on a minimum distance rule and the constraints on spectral parameters and spatial thresholds were constructed. In the minimum distance estimation, for separation of the classes, only pixels falling within 1.0 standard deviation (SD) (these pixels more clearly represented the related class) and the features extracted through a feature extraction process, were used. To extract the reliable features in which the selected classes could be separable, the principal components (PC) extracted through the principal component analysis (PCA) and the Pauli components defined from the Pauli matrix basis (Ferro-Famil *et al.* 2001), were compared. The analysis indicated that the available classes were more separable in 3 features extracted from the PCA than in 6 features obtained

from the Pauli matrix basis. The PCA has been performed using each of the X-band and L-band data separately. The results are shown in Table 1a,b.

a)

	PC1	PC2	PC3
Xhh	0.57	0.45	-0.68
Xhv	0.57	-0.81	-0.05
Xvv	0.58	0.35	0.72
Variance (%)	89.88	6.82	3.3

b)

	PC1	PC2	PC3
Lhh	0.57	0.73	-0.36
Lhv	0.57	-0.67	-0.46
Lvv	0.58	-0.05	0.80
Variance (%)	88.19	8.23	3.58

Table 1. Principal component coefficients.
(a) from Pi-SAR X-band data
(a) from Pi-SAR L-band data.

As seen from the Table 1a,b, in both data sets, the PC1 contains over 88% of the overall variance and equally dominated by the variance of all polarization components, while in the PC2 the cross polarization components have high negative loadings. Moreover, it can be seen that the first 2 PCs contain over 96% of the overall variance. The inspection of the last PCs in both bands indicated that they contained noise from the total data set.
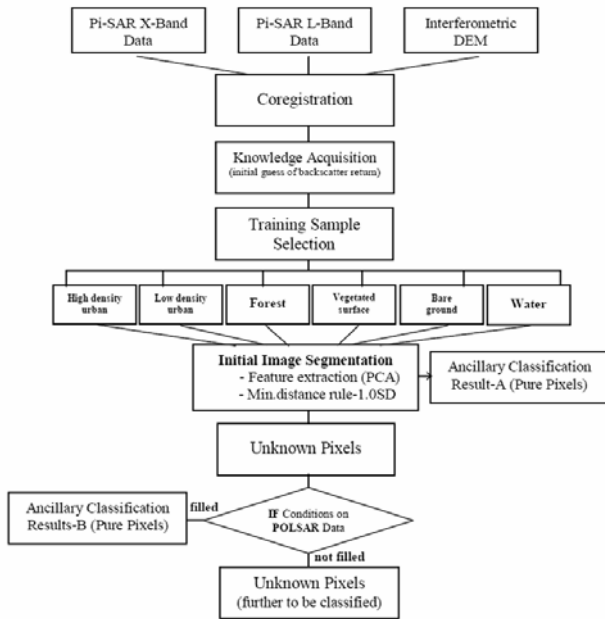

Figure 3. The flowchart showing the classification procedure used in the upper hierarchy.

For the final features, X-PC1, L-PC1 and the average of the PC2 of both bands were selected. These selected features were evaluated using the minimum distance rule. The decision rule can be written as

$$d_j(x) = (x - m_j)^t (x - m_j) \qquad (1)$$

and if $SD(x) \geq 1.0$, then a pixel (x) is assigned to the class (C_j) where d_j is minimum and the pixels falling outside of 1.0 SD

were temporarily identified as unknown classes and further classified using the rules in which different spectral and spatial thresholds were used. The flowchart for this classification procedure is shown in Figure 3.

As can be seen from the initial knowledge acquisition process, there are different statistical overlaps among the classes, but significant overlaps exist between the classes low density urban and forest as well as between the classes bare ground and water. In the lower hierarchy of the rule-base, different rules for separation of these overlapping classes were constructed using different spectral and spatial thresholds. In general, it is very difficult to separate the classes if they have the same or very similar spectral characteristics. In such a case, the usage of thoroughly defined spectral and spatial thresholds can play an important role for separating the overlapping classes. The spectral thresholds can be defined from the statistics of the training signatures of the available classes, while the spatial thresholds can be determined on the basis of historical data sets stored within a GIS or from local knowledge about the site. In this study, the spatial thresholds were defined based on local knowledge about the test area.

For separation between the classes low density urban and forest, a rule based on a non-parametric approach which uses both spectral and spatial thresholds was constructed, while for separation between the classes bare ground and water, a rule based on a spatial threshold defined from the InDEM was used. In order to define the spatial threshold from the InDEM, the river valley had to be clearly separated from the surroundings and for this aim, different texture filters based on occurrence and co-occurrence measures were applied. By applying these measures, initially 9 texture features have been obtained, but after thorough checking of each individual feature only 3 features including the results of the mean, data range and variance filters were selected (Gonzalez and Woods, 2002). After that, the river valley was extracted using a rule in which spectral thresholds were applied. In the selected test site, some parts of the mountainous areas have very steep slopes and the areas located below such slopes are highly affected by radar shadows. The effect of radar shadow can be reduced (or eliminated) by the use of either filtering or masking. The filtering may be successfully used if there is a little shadow. However, it has less effect if there is a large shadow and an alternative method could be a usage of different masks. In the present study, for the elimination of the existing shadows, the masks defined on the basis of local knowledge have been applied. The flowchart for the classification procedure in the lower hierarchy of the rule-base is shown in Figure 4.
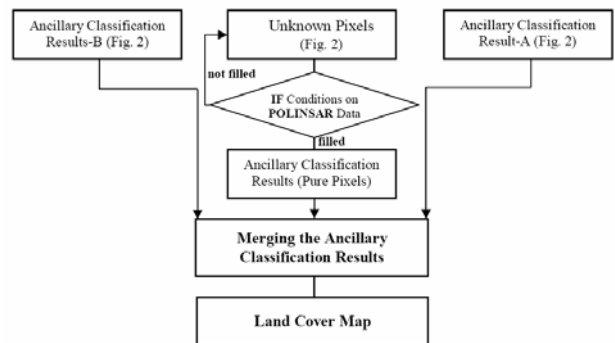

Figure 4. The flowchart showing the classification procedure used in the lower hierarchy.
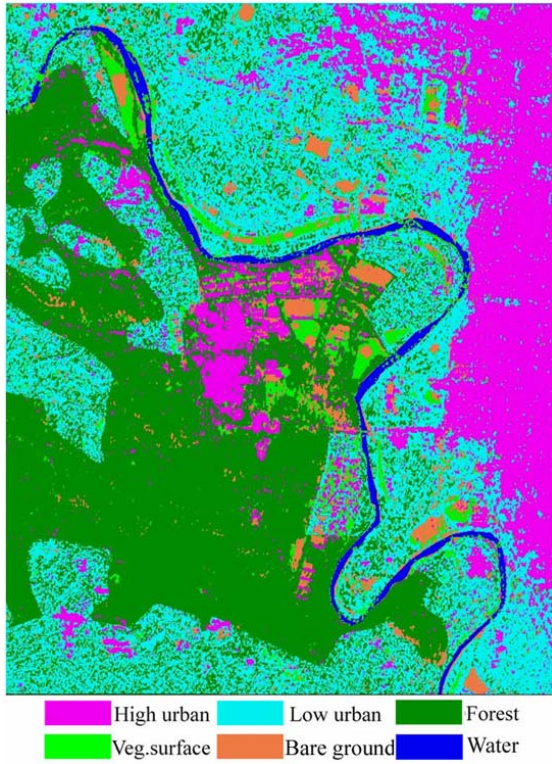
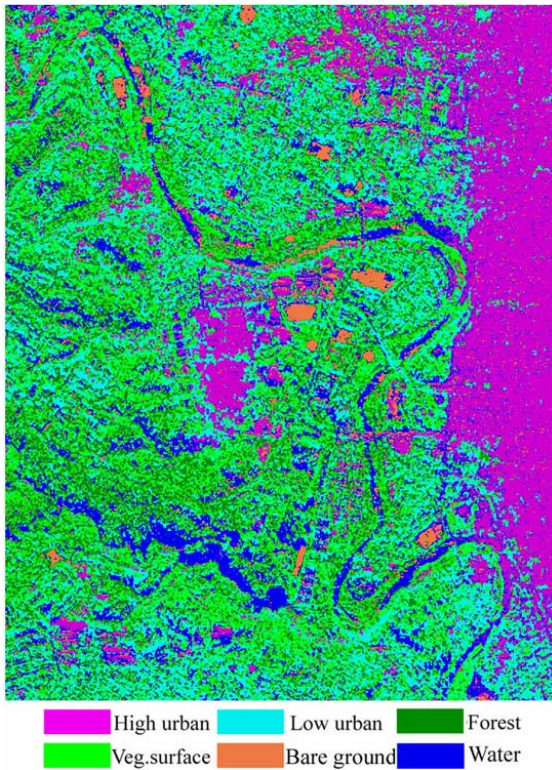Figure 5. The classified image using the rule-based algorithm.

Figure 6. The classified image using the statistical MLC method.

The image classified by the developed method is shown in Figure 5. For the accuracy assessment of the classification result, the overall performance has been used. As ground truth information, the regions containing the total of 35774 purest pixels have been selected. The confusion matrix indicated an overall accuracy of 91.33% (Table 2).

To compare the performances of the developed algorithm and a standard method, the same set of features and training signatures used for the rule-based classification, were classified using the statistical MLC. The image classified by the MLC method is shown in Figure 6. The confusion matrix indicated an overall accuracy of 57.18% (Table 3).

Classified data	Reference data					
	1	2	3	4	5	6
1	11096	158	124	0	0	0
2	708	10226	657	0	65	0
3	126	862	9478	84	0	0
4	0	0	0	925	0	26
5	0	0	0	289	761	0
6	0	0	0	0	0	189
Total	11930	11246	10259	1298	826	215
Overall Accuracy = (32675/35774) 91.33%						

Table 2. Confusion matrix produced for the rule-based classification (1-high density urban, 2- low density urban, 3- forest, 4- vegetated surface, 5- bare ground, 6- water).

Classified data	Reference data					
	1	2	3	4	5	6
1	10989	117	0	0	0	21
2	812	4126	86	16	46	0
3	105	2997	3756	252	40	12
4	0	3628	5514	902	37	28
5	0	0	0	71	579	52
6	24	378	903	57	124	102
Total	11930	11246	10259	1298	826	215
Overall Accuracy = (20454/35774) 57.18%						

Table 3. Confusion matrix produced for the statistical MLC (1-high density urban, 2- low density urban, 3- forest, 4- vegetated surface, 5- bare ground, 6- water).

5. CONCLUSIONS

The aim of this research was to demonstrate the use of the Pi-SAR data for the extraction of different thematic information used for urban planning and management. For this end, different terrain topography related thematic information as well as a land cover map were generated from the Pi-SAR data. The terrain related thematic maps such as slope, aspect, contour and shaded relief maps as well as various convexities and curvatures were generated from the InDEM by applying standard procedures, while for the generation of the land cover map, a refined classification algorithm, which can integrate both polarimetric and interferometric information was developed. The refined method was based on a hierarchical rule-based approach and it used a hierarchy of rules describing different conditions under which the actual classification should be performed. In the lower hierarchy, based on the knowledge about scattering characteristics of the selected classes, a set of rules which contains the initial image segmentation procedure and the constraints on the spectral parameters and other

threshold values were constructed. The rules in the upper hierarchy include different constraints on spectral thresholds defined from POLSAR data and spatial thresholds defined from the interferometric information. The result of the developed method was compared with the result obtained by the traditional MLC method and it demonstrated better performance than this method.

ACKNOWLEDGEMENTS

REFERENCES

Amarsaikhan, D., 2000. Application of spectral and scattering knowledge for interpretation of active and passive sensor data. Institute of Informatics and RS, Mongolian Academy of Sciences, Report TR-00-18, Ulaanbaatar, Mongolia.

Amarsaikhan, D. and Sato, M., 2003. The role of high resolution satellite images for urban area mapping in Mongolia. In: *"Reviewed Papers" part of CD-ROM Proceedings of the CUPUM'03 Conference*, Sendai, Japan, May 2003, pp. 1-12.

Amarsaikhan, D. and Sato, M., 2004. Validation of the Pi-SAR data for land cover mapping. *Journal of the Remote Sensing Society of Japan,* No.2, Vol.24, pp.133-139.

ENVI, 1999. User's Guide. Research Systems, USA.

ERDAS, 1999. Field guide. 5th Ed. ERDAS, Inc. Atlanta, Georgia, USA.

Ferro-Famil, L., Pottier, E. and Lee, J. S., 2001. Unsupervised classification of multifrequency and fully polarimetric SAR images based on the H/A/Alpha–Wishart classifier. *IEEE Trans. Geosci. Remote Sensing.* vol. 39, pp. 2332–2342.

Gonzalez, R. C. and Woods, R. E., 2002. *Digital Image Processing.* 2nd ed. Upper Saddle River, New Jersey: Prentice-Hall.

Lawrence, L. and Wright, A., 2001. Rule-based classification systems using classification and regression tree (CART) analysis. *Photogramm. Eng. Remote Sens.*, vol. 67, pp. 1137–1142.

Manual of Remote Sensing, 1998. 3rd ed. vol. 3, American Society of Photogrammetry.

Richards, J. A., 1993. *Remote Sensing Digital Image Analysis-An Introduction*, 2nd ed. Berlin: Springer-Verlag.

Satake, M., Uratsuka, S., Umehara, T., Maeno, H., Nadai, A., Kobayashi, T., Matsuoka, T., Manabe T. and Masuko, H., 2002. Flight experiments of airborne high-resolution multi-parameter imaging radar, Pi-SAR. *Journal of the Communications Research Laboratory,* vol. 49, no. 2, pp. 127-141.